Microenvironmental reprogramming by three-dimensional culture enables dermal papilla cells to induce de novo human hair-follicle growth

Claire A. Higgins[a], James C. Chen[b,c], Jane E. Cerise[a], Colin A. B. Jahoda[d,1], and Angela M. Christiano[a,b,1]

Departments of [a]Dermatology, [b]Genetics and Development, and [c]Systems Biology, Columbia University, New York, NY 10032; and [d]School of Biological and Biomedical Sciences, Durham University, Durham DH1 3LE, United Kingdom

This Feature Article is part of a series identified by the Editorial Board as reporting findings of exceptional significance.

Edited by Zena Werb, University of California, San Francisco, CA, and approved September 5, 2013 (received for review May 28, 2013)

De novo organ regeneration has been observed in several lower organisms, as well as rodents; however, demonstrating these regenerative properties in human cells and tissues has been challenging. In the hair follicle, rodent hair follicle-derived dermal cells can interact with local epithelia and induce de novo hair follicles in a variety of hairless recipient skin sites. However, multiple attempts to recapitulate this process in humans using human dermal papilla cells in human skin have failed, suggesting that human dermal papilla cells lose key inductive properties upon culture. Here, we performed global gene expression analysis of human dermal papilla cells in culture and discovered very rapid and profound molecular signature changes linking their transition from a 3D to a 2D environment with early loss of their hair-inducing capacity. We demonstrate that the intact dermal papilla transcriptional signature can be partially restored by growth of papilla cells in 3D spheroid cultures. This signature change translates to a partial restoration of inductive capability, and we show that human dermal papilla cells, when grown as spheroids, are capable of inducing de novo hair follicles in human skin.

The growth and unique cycling activities of the hair follicle is largely controlled by a group of specialized mesenchymal cells, located in a structure termed the dermal papilla. The precursors of papilla cells are mesenchymal-cell aggregations, or condensates, that form in embryonic skin dermis at the start of follicle morphogenesis (1). These aggregations are necessary for hair-follicle development because their early dispersal leads to a disruption of hair-follicle formation (2). It is within the mesenchyme (dermis) that the initiating signal for hair-follicle development is believed to arise (3, 4). Subsequent stages of hair-follicle morphogenesis are then orchestrated by reciprocal interactions between the mesenchyme and overlying epithelium, with numerous genetic studies identifying the key developmental pathways involved in this process (5). These morphogenetic events occur before birth, with hair-follicle neogenesis in the adult believed to recur only in extreme circumstances, such as after wounding (6).

Remarkably, over 40 y ago, it was demonstrated that adult rodent dermal papillae can be removed from the hair follicle and transplanted in their intact state into recipient skin, where they induce de novo follicle development and hair growth (7, 8). These experiments demonstrated that dermal papillae, unlike fibroblasts, can reprogram non-hair-bearing epidermis to a follicular fate, recapitulating the events of embryonic hair morphogenesis. Subsequent studies have demonstrated that these inductive properties are maintained in early rodent dermal papilla cell cultures because these cells are also capable of inducing new hair follicles and hair fibers in recipient epithelium (9–11).

In attempting to establish a cell transplantation approach for human hair-follicle neogenesis, investigation has focused on showing that human dermal papilla cells have the same inductive properties as rodent cells. However, despite a strong translational interest in the process termed "hair-follicle cloning" (12, 13), as well as our earlier demonstration that intact human hair-follicle dermal sheath tissue is inductive (14, 15), subsequent efforts to elicit human follicle neogenesis with cultured human hair-follicle dermal cells in human skin have not been successful.

When dermal papilla cells are removed from their hair-follicle microenvironment and grown in culture, they immediately lose contextual and positional cues from the surrounding epithelial cells. During the course of extended primary cell culture, rodent cells lose their inductivity, but this property can be restored if appropriate epithelial influences are provided (16). These cues can be mimicked in part by specific molecular entities; for example, Wnt and BMP signals have been shown to prolong hair-follicle inductivity in cultured rodent papilla cells (10, 11, 17). Similar strategies have been attempted with cultured human dermal papilla cells, including the addition of soluble factors, or using keratinocyte-conditioned medium in attempts to restore the contextual epithelial influence (18, 19). However, translating these successful rodent experiments into the human system has been a rate-limiting step with this approach. Up to now, the key demonstration of cultured human dermal papilla cells inducing hair neogenesis specifically in the context of human skin has not been accomplished.

Significance

Growth of de novo hair follicles in adult skin occurs by a process known as hair neogenesis. One way of initiating neogenesis is to place dermal papillae isolated from the hair follicle in contact with an overlying epidermis where they reprogram the epidermis to adopt a follicular fate. This approach, however, has not been successful using cultured human dermal papilla cells in human skin because the cells lose their ability to induce hair growth after expansion in vitro. In this paper, we demonstrate that by manipulating cell culture conditions to establish three-dimensional papilla spheroids, we restore dermal papilla inductivity. We also use several systems biology approaches to gain a comprehensive understanding of the molecular mechanisms that underlie this regenerative process.

Author contributions: C.A.H., C.A.B.J., and A.M.C. designed research; C.A.H., J.C.C., and J.E.C. performed research; C.A.H., C.A.B.J., and A.M.C. analyzed data; and C.A.H., C.A.B.J., and A.M.C. wrote the paper.

The authors declare no conflict of interest.

This article is a PNAS Direct Submission.

Data deposition: The data reported in this paper have been deposited in the Gene Expression Omnibus (GEO) database, www.ncbi.nlm.nih.gov/geo (accession no. GSE44765).

See Commentary on page 19658.

[1]To whom correspondence may be addressed. E-mail: amc65@columbia.edu or colin.jahoda@durham.ac.uk.

This article contains supporting information online at www.pnas.org/lookup/suppl/doi:10.1073/pnas.1309970110/-/DCSupplemental.

One striking difference between the behavior of human scalp dermal papilla cells and those of rodent vibrissa follicles is their propensity and capacity to aggregate both in vitro and in vivo. Indeed, this intriguing cell-autonomous property is observed in cultured rat dermal papilla cells after subdermal injection, suggesting that they maintain their identity even after they are transplanted in the absence of epidermal contact. The cultured rat dermal papilla cells self-aggregate within the dermis, adopting embryonic-like properties, and form a papillae condensate-like clump that synthesizes its own extracellular matrix (20). However, we have never observed spontaneous aggregation in cultured human dermal papilla cells injected into skin, highlighting species-specific differences related to self-aggregative behavior. Intriguingly, these observations invite a different strategy for achieving the necessary first step toward human hair follicle neogenesis, i.e., promoting cultured human dermal papilla cells to undergo self-aggregation.

To dissect the molecular events underlying the loss of induction in human cells, in this study, we defined the transcriptome of dermal papilla cells as they lose their inductive capacity. Global microarray profiling demonstrated that perturbation of human dermal papilla cells by growth in standard monolayer cell culture dramatically altered their transcriptional profile. Unexpectedly, the most significant changes in the papilla transcriptome occurred after only a brief period of culture initiation, accounting for the rapid loss of their capacity for hair-follicle induction. It is widely known from other biological disciplines that growth of cultured cells in 2D culture imposes highly unnatural constraints on cells that can dramatically alter cellular behavior (21). To overcome this limitation of 2D culture, we used spheroid aggregate cultures (22) because they reliably resemble in vivo structure of other tissues, both morphologically and biochemically (23).

We show here that, by creating the microenvironment for self-aggregation by culturing dermal papilla cells in hanging drop cultures, we establish dermal spheroids that physiologically mimic cell condensations. Creating 3D spheroids partially restored the intact dermal papilla gene-expression signature within the cells and, in turn, their associated hair-inducing properties. Microsurgical implantation of dermal spheroids in a unique human skin induction assay enabled us to demonstrate that the establishment of dermal papilla cells in spheroids is, in itself, sufficient to partially restore inductive properties to cultured dermal papilla cells.

Here, we show that cultured human dermal papilla cells are capable of inducing human follicle formation when implanted into human skin, providing a proof-of-concept study. These observations represent a significant advance in using cell-based therapy for hair-follicle neogenesis, bringing it closer to becoming a therapeutic reality.

Results

Intact Human Papillae, but Not Cultured Cells, Are Capable of Neogenesis. First, to determine the conditions for human hair-follicle neogenesis, we established a unique contextual human hair induction assay using dermal papillae implanted into human skin. Neonatal foreskin was selected as non-hair-bearing recipient tissue because it would challenge the human dermal papillae not just to contribute to hair follicles within the skin, but rather, to fully reprogram the recipient epidermis to a follicular fate. Intact dermal papillae were microdissected from adult human hair follicles and placed between the epidermis and dermis of dispase-separated foreskin tissue. On two occasions, recombined tissue, containing papillae from different male donors, was grafted onto the back of a SCID mouse for 6 wk (nine papillae from donor D1 and seven papillae from donor D2). When intact dermal papillae were used as a positive control, we observed that several hair follicles had been induced within the grafts after 6 wk (Fig. 1*A*). These follicles were comprised of human cells, as shown using an antibody specific to human nuclei (Fig. 1*B*). This antibody was expressed in cells in the same expression pattern as follicles of human control skin. Hair follicles have concentric epithelial layers, which surround and support the growing hair shaft. Using antibodies specific for keratins present in these layers, we detected a regular epithelial configuration within the new appendages, demonstrating that intact dermal papillae are capable of inducing normal human hair follicles in recipient epidermis (Fig. 1 *C* and *D*). In contrast, when a slurry of dermal papilla cells (donors D3 and D4) cultured under normal 2D conditions was inserted between the recombined epidermis and dermis, no hair follicle induction was observed after 6 wk (Table S1). One explanation is that the 3D context in which the dermal papilla usually resides is lost when the cells are grown in 2D cultures.

Perturbation by in Vitro Growth Alters the Dermal Papilla Transcriptome. To determine the transcriptional events underlying the loss of inductivity, we used Affymetrix microarrays to perform profiling of dermal papilla cells, both as intact tissues, and at the following stages in subsequent 2D culture: cell explant outgrowths (p0) and cells at passage 1 (p1), passage 3 (p3), and passage 5 (p5) (GEO accession no. GSE44765). All experiments were performed using three biological replicates (donors D5, D6, and D7), using RNA isolated from the papilla cells of three male donors (aged 32, 34, and 37). Using GeneSpring, we performed a one way ANOVA on the dataset to identify 10,653 transcripts that were significantly ($P < 0.05$) and differentially (fold change >2) regulated between intact isolated dermal papilla and cells at subsequent culture stages (p0, p1, p3, and p5). Graphical representation of the data clearly illustrated that the most dramatic changes to the transcriptome occurred between intact papillae and the early outgrowths of papilla cells, with subsequent growth and passaging

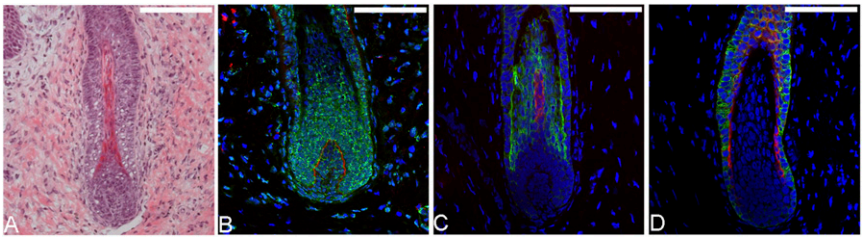

Fig. 1. Human hair neogenesis instructed by intact dermal papillae. (*A*) Intact human dermal papillae induced de novo follicle growth in recipient tissue as determined by hematoxylin/eosin staining. (*B*) A human-specific antibody (green) shows the presence of human cells throughout new hair follicles whereas laminin 5 (red) demarcates the newly formed basement membrane. DAPI (blue) marks all cells. (*C*) Keratin 71 (green) marks the inner root sheath whereas Keratin 31 (red) marks the hair cortex of new hair follicles. (*D*) Keratin 14 (green) shows the presence of outer root sheath whereas Keratin 75 (red) marks the companion layer. (Scale bars: 100 μm.)

eliciting far fewer alterations (Fig. 2*A*). When we performed a *t* test to identify significant differences between intact dermal papilla and only cells at p0, the list of significantly and differentially expressed genes contained 3,729 transcripts. The most highly differentially expressed of these (the top 80 transcripts increasing in expression, and top 80 decreasing in expression) are displayed in Table S2. Using real-time PCR, we validated and quantitated (Fig. 2*B*) the observed expression changes in a number of transcripts [*clusterin* (*CLU*), *endothelin 3* (*EDN3*), *low density lipoprotein receptor-related protein 4* (*LRP4*), *wnt inhibitory factor 1* (*WIF1*), *adenomatosis polyposis coli down-regulated 1* (*APCDD1*), *lymphoid enhancer-binding factor 1* (*LEF1*), *chemokine* (*C-X-C motif*) *receptor 4* (*CXCR4*), *matrix gla protein* (*MGP*), and *gremlin 1* (*GREM1*)], including several that have been previously implicated as having an important role during hair-follicle development (24, 25). Additionally, with immunofluorescence, we localized expression of proteins within intact dermal papilla that decreased in expression in culture (Fig. S1). The large number of transcripts identified as differentially expressed between intact papilla versus cells early in culture (p0) highlights the profound impact that being initiated into 2D culture has on the molecular signature of papilla cells. The remarkable speed of this environmental deprogramming also provides an explanation as to why the inductivity of human dermal papilla cells is lost rapidly after entering monolayer culture.

We next performed an unbiased global analysis of intact papillae versus cells at p0 using iPAGE software (26). Transcripts were separated into 20 expression bins based on their log expression ratios between intact papillae and p0 cells while iPAGE then uses mutual information to compare expression and pathway profiles. Gene ontology terms for "mitotic cell cycle," "DNA replication," and "translation initiation" were most highly overrepresented within p0 cells (Fig. 2*C*). From the iPAGE analysis, it was evident that, once intact dermal papillae were placed into culture, the geometric and mechanical alterations imposed on the cells, in addition to the presence of a growth factor-rich serum in the culture medium, resulted in transcription of genes associated primarily with cell division and metabolism. Both of these transcriptional networks represent departures from the normal homeostatic conditions observed in intact dermal papillae. Interestingly, at the other end of the spectrum, the gene ontology term for the "Wnt receptor signaling pathway" was underrepresented in cultured cells, but overrepresented in intact dermal papilla. The Wnt signaling pathway has been shown to be

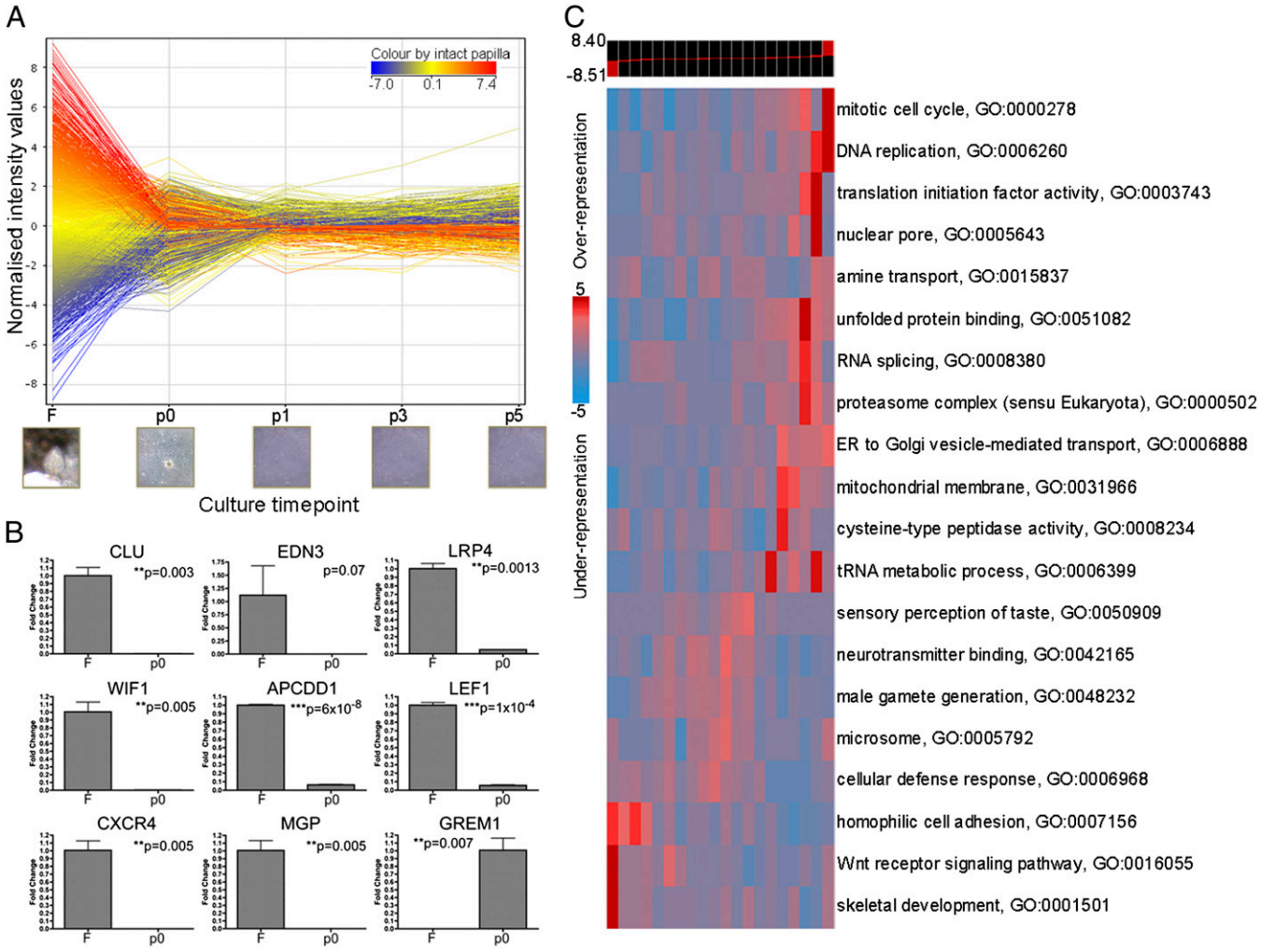

Fig. 2. Rapid loss of the dermal papilla transcriptome by growth in vitro. (*A*) Profile plot of dermal papilla culture. Each line represents a transcript that was both significantly and differentially regulated between intact papilla (F), and cells at different time points in culture, from explants (p0), through to passaged cells (p1, p3, p5). (*B*) Semi-quantitative real-time PCR results showing differences between freshly isolated papillae (F) and papilla cell explants (p0). (*C*) Global iPAGE analysis showing over- and underrepresented gene ontology terms. Expression bins divide transcripts, with bins on the left containing genes highly expressed within intact papillae and those on the right containing genes up-regulated within cells at p0.

crucial for hair-follicle morphogenesis (27); thus, it is likely that perturbation of this signaling pathway has a crucial effect on the observed loss of inductive potential seen in the papilla cells once they are grown in vitro.

Three-Dimensional Culture Partially Restores Hair Follicle Inductivity in Dermal Papilla Cells. Three-dimensional culture models have been shown to recapitulate their in vivo tissue counterparts by reestablishing the tissue microenvironment that promotes an appropriate cellular phenotype (28). To reverse the changes that occurred in 2D culture (Fig. 3*A*), dermal papilla cells (passages p3, p4, and p5) from seven separate donors (independent from the microarray donors) were grown in hanging drop cultures to establish spheroids containing ∼3,000 cells (Fig. 3*B*) Spheroids formed readily by 24 h and were morphologically akin to intact dermal papilla (22). Per experiment, between 10 and 15 spheres were placed between separated foreskin epidermis and dermis, which was recombined and grafted onto SCID mice. Strikingly, after 6 wk, we observed de novo hair follicles (Fig. 3*C*) from five of the seven donors (Table S3, Fig. S2), which we confirmed were comprised of human cells using an antibody specific to human nuclei (Fig. 3*D*). On two occasions, unpigmented hair shafts were observed emerging from the skin that had been implanted with spheroids (Fig. 3*E*). Sebaceous glands were not seen in follicles created after spheroid transplantation whereas these glands were detected in follicles induced by transplanted intact dermal papillae. Histological analysis of the sectioned skin showed that the induced hairs clustered together, most likely due to the close proximity of spheres when they were placed in the graft (Fig. S2). Grafts analyzed after only 5 d, instead of 6 wk, revealed areas where several spheres were beginning to coalesce as a single condensate structure (Fig. S2). At this early time point, however, positive staining of placode markers in the overlying epidermis was not observed.

In the de novo hair follicles, the newly induced papilla and sheath were highly positive for alkaline phosphatase (Fig. 3*F*), readily distinguishing them from surrounding fibroblasts. Moreover, hair-specific keratin markers delineated all concentric epithelial layers in the induced follicles (Fig. 3 *G* and *H*). We were also able to visualize mouse blood-vessel formation, particularly around de novo follicles, indicating anastomosis with the graft (Fig. 3*I*). Additionally, we used laser capture microdissection to perform molecular fingerprinting using two microsatellite markers and confirmed that the dermal papilla in de novo hair follicles were not only human, but were specifically of donor origin (Fig. 3*J*).

The longest duration of any graft in our study was 6 wk, and therefore long-term follicle function was not assessed. At this endpoint, the efficiency of inductivity varied between donors, ranging from 10% to 60%. Importantly, however, spheroids from donors whose cells proved to be inductive in an initial experiment were able to robustly and reproducibly induce follicles in every experimental replicate (Table S3). This reproducibility emphasizes that interindividual differences may contribute to the variable inductive potential of spheroids, rather than the variability in the assay itself.

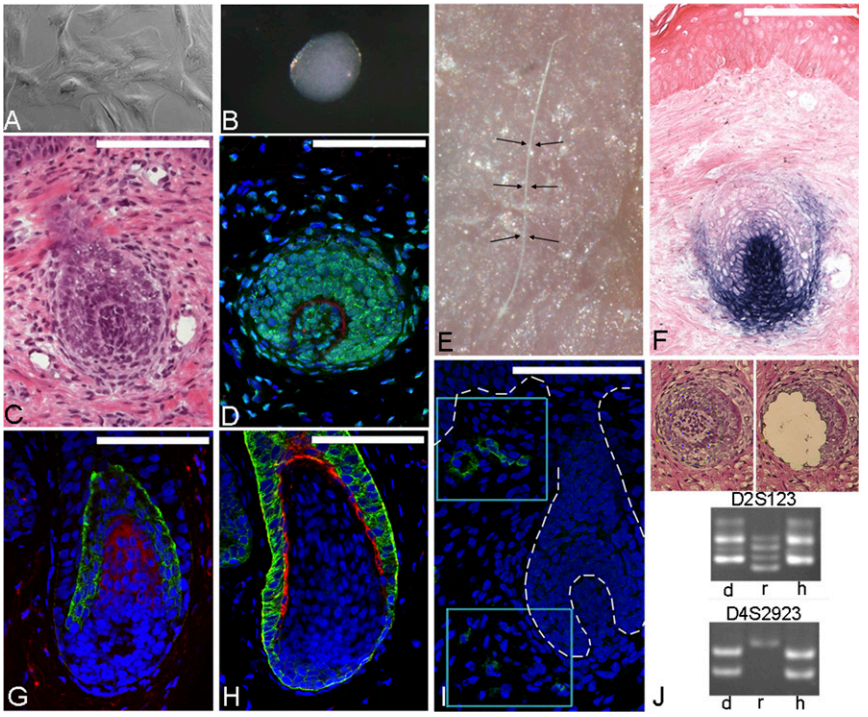

Fig. 3. Human hair follicle neogenesis instructed by papilla spheroids. (*A*) Dermal papilla cells grown in regular flat culture conditions. (*B*) A dermal papilla spheroid, established after a 30-h hanging drop culture. (*C*) Haematoxyin/eosin histology of hair-follicle induction in recipient foreskin tissue. (*D*) A human-specific antibody (green) shows human cells throughout a de novo follicle whereas laminin 5 (red) demarcates the new basement membrane separating the papilla and matrix, and DAPI (blue) marks all cell nuclei. (*E*) Macroscopic view of unpigmented hair shaft (between arrows) protruding from experimental foreskin tissue 6 wk post grafting. (*F*) Alkaline phosphatase staining of the newly formed dermal papilla and sheath. (*G*) Keratin 71 (green) labels inner root sheath whereas Keratin 31 (red) labels the hair cortex of induced hair follicles. (*H*) Keratin 14 (green) demarcates the outer root sheath whereas Keratin 75 (red) shows the presence of a companion layer in new hair follicles. (*I*) Within our human skin grafts, we observed mouse CD31 (green) expression, particularly around the de novo follicles in both the areas near the bulge, and the bulb (boxed regions). Basement membrane delineating hair follicle is outlined with white dashes. (*J*) Image showing laser-captured tissue and subsequent gel images of microsatellite marker analysis demonstrates that donor spheres share a molecular fingerprint with hair follicles in recipient tissue. d, donor spheres; h, dermal papilla in novel hair induction assay; r, recipient tissue. (Scale bars: 100 μm.)

Three-Dimensional Culture Partially Restores the Intact Dermal Papilla Signature. To understand the molecular events driving the partial restoration of inductivity in spheroids, we conducted Affymetrix microarray profiling on 48 h spheroids. We identified transcriptome signatures for dermal spheroids established from the same three male donors as the previously profiled dermal papilla cells (donors D5, D6, and D7). We performed unsupervised hierarchical clustering on the whole-genome signatures of intact papilla, cells from p0–p5 in culture, and dermal spheroids and found that, whereas intact papillae from each donor clustered together, spheroids were clustered independently from the remainder of the cells in 2D cultures (Fig. 4*A*). Because cells at p3 were used to establish spheroids, we used the list of transcripts differentially expressed between intact papillae and p3 cells to calculate correlation among intact papillae, p3 cells, and spheroids. The average correlation coefficient between intact dermal papilla and cells at p3 was 0.42 (range: 0.39–0.44) whereas between intact papillae and spheroids it was 0.56 (range, 0.55–0.58) (Fig. 4*B*). We determined that this increase in correlation coefficient between intact dermal papillae and dermal spheroids equates to a partial restoration of an intact dermal papillae signature by 3D culture. Approximately 22% of transcripts perturbed

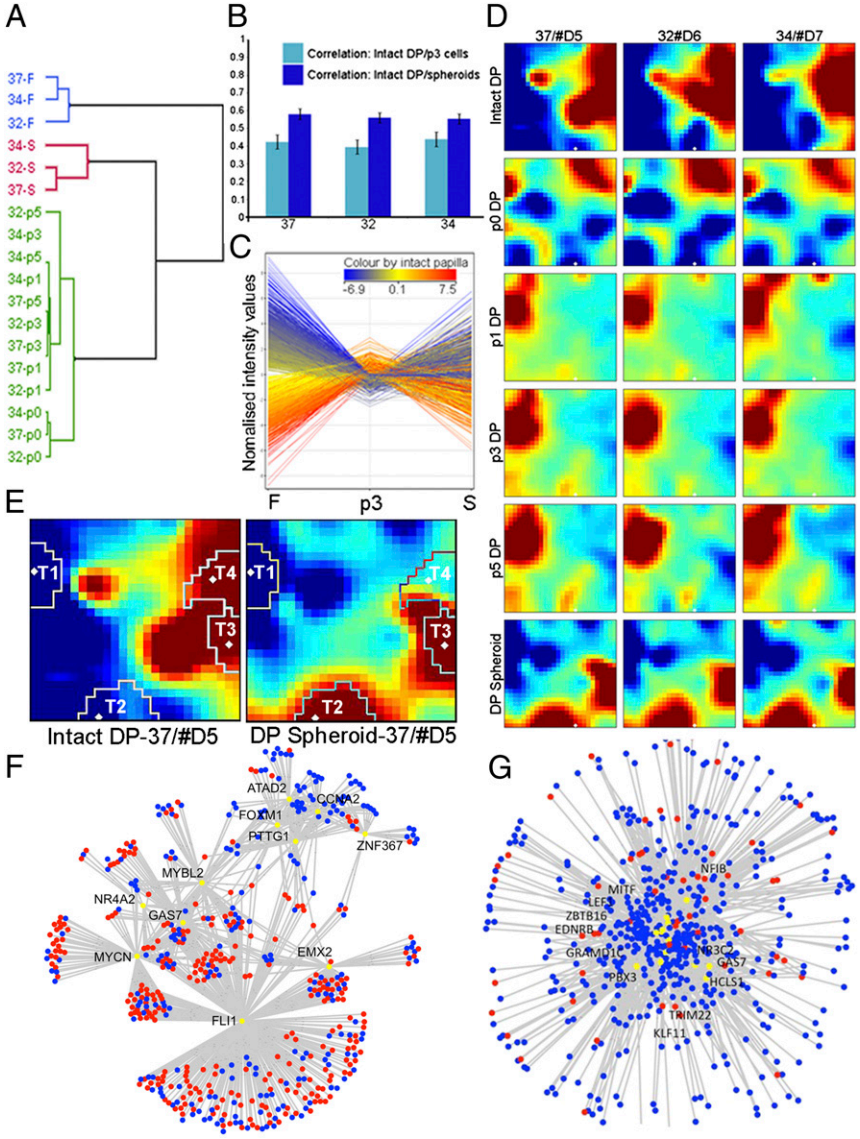

Fig. 4. Restoration of in vivo signature by reassembly of dermal papilla cells into spheroids. (*A*) Dendrogram of an unsupervised hierarchical cluster performed on global profiles of intact papillae (blue), cells in culture (green), and dermal spheroids (red). Arrays are identified by patient age. (*B*) Bar chart comparing similarity of intact papilla with p3 cells, or p3 spheroids, plotted as Pearson's correlation coefficients. Individual samples are identified by age of tissue donor (37, 32, 34 y). (*C*) Profile plot comparing intact papillae (F), cells at p3, and spheroids (S) shows that 22% of transcripts differentially regulated between intact papillae and cells at p3 were restored by reassembly into spheroids. (*D*) GEDI global analysis among microarrays of fresh papillae, cells in culture (p0, p1, p3, p5), and spheroids. Expression values of each probe set, for each sample, were input into a 25 × 26 node grid, whereby changing expression patterns within intact dermal papillae can be assessed as a genome-wide response to growth in culture. (*E*) GEDI analysis revealed four territories of interest (T1–T4), in which the dynamics of expression changes among samples were of particular interest. (*F*) Network presentation of transcription factors (yellow nodes) with significant enrichment of genes in territories 1 + 3, or in territories 2 + 4 (*G*). Red nodes denote territories 1 and 2 in their respective regulons, and blue nodes denote territories 3 and 4. Several transcription factors were detected; however, the transcription factor FLI1 was identified as a regulator unique to the biomarker panel of both territories 1 and 3 and a significantly larger portion of the territory genes than other candidates. In analyzing territories 2 + 4, several significant master regulators were identified with comparable effect sizes, and are indicated within the figure.

by 2D culture were restored toward the levels of expression in intact papillae, by growth as spheroids (Fig. 4*C*).

The observation of hair follicles within grafts, as described above, suggests that the 22% restoration of papilla signature is sufficient for follicle neogenesis. However, as complete hair-follicle morphogenesis involves epithelial:mesenchymal interactions, it is likely that external paracrine signals will be required for full signature restoration and development of external hairs. Importantly, in this study, we have demonstrated that dermal spheroids are, by themselves, capable of initiating the hair induction process in non-hair-bearing human skin, where there are no previous epidermal "hair-follicle" signals.

To further explore the dynamics of the changing expression profile observed within our samples we used the computational algorithm GEDI (The Gene Expression Dynamics Inspector), which enables visual representation of large datasets (29). Genes are grouped into metagene categories based on their temporal expression profiles and placed into 1 of 650 metagenes on a 25 × 26 grid. Although individual differences between cell donors (donors D5, D6, and D7) in each category were small, we observed differences between the dermal papilla cells in different cell states (Fig. 4*D*). There were four particular regions of interest within the dataset that we designated territories T1–T4 (Fig. 4*E*, Tables S4–S7). Both T1 and T3 contained metagenes whose expression was deregulated in culture from intact papillae (Fig. S3) but were restored by growth of cells in spheroids, equating to our previously identified 22% restoration signature. Particularly within the T3 territory, a number of genes were identified that have previously been associated with the intact dermal papilla signature, including *HEY1*, *bone morphogenetic protein 2* (*BMP2*), *fibroblast growth factor 7* (*FGF7*), and *secreted frizzled related protein 2* (*SFRP2*) (30, 31). Within the T1 territory, genes including *αSMA*, *GREM1*, and *FZD6* were identified, that increased in expression in 2D culture but decreased to in vivo levels in a 3D environment. Using immunofluorescence to assess both 2Dly cultured cells and dermal papilla spheroids, we visualized changes in POSTN and HAS2 protein expression, corresponding to the changing gene levels in the T1 territory, and changes in BMP2, SFRP2, MGP, and A2M, corresponding to the T3 territory (Fig. S4).

In contrast to T1 and T3, territories T2 and T4 contained metagenes that were either increased or decreased by growth in culture but were not restored by spheroid culture, showing a divergence from the intact papillae expression profile. T4 was of particular interest because it included genes such as *sclerostin domain containing 1* (*SOSTDC1*), *WIF1, LEF1*, and *CD133,* all of which have previously been implicated in hair growth (32–34). WIF1 is a Wnt inhibitor whereas SOSTDC1 is both a Wnt and Bmp antagonist. Interestingly, another BMP inhibitor, *GREM1*, was increased in expression, and was identified in territory T1 as mentioned above. This increase in expression of *GREM1* in culture may explain the decreased expression of BMPs 2, 4, 5, and 7 in the cultured dermal papilla cells. In spheroids, *GREM1* expression decreased whereas *BMP2* and *BMP4* expression was increased. However, *BMP5* and *BMP7* expression was not restored by spheroid culture. BMPs have been previously shown to have a fundamental role during hair development and hair cycling (35–37) whereas BMP6 treatment of mouse dermal papilla cells can enhance their hair-inducing capacity (11).

We further interrogated the initial 22% of restored transcripts (territories T1 and T3), using the systems biology algorithm Panther (38) to identify protein classes that are both over- and underrepresented within our list, compared with representation of these protein classes within the entire human genome. Similar results were obtained using either the subset of genes in the original 22%, or in the T1 and T3 territories. Using Panther, several protein classes were identified as being overrepresented within dermal spheroids, of which only those exceeding significance ($P < 0.05$) were displayed graphically (Fig. S5). The most significant included extracellular matrix structural proteins ($P = 1.5 \times 10^{-7}$), extracellular matrix proteins ($P = 8.2 \times 10^{-7}$), and signaling molecules ($P = 2.5 \times 10^{-5}$). The extracellular matrix category included several collagens, such as *FBLN1*, *COL23A1*, and *MGP* in addition to other transcripts that are expressed in the intact dermal papilla (18). Within the signaling class, key secreted factors such as *FGF7* and *BMP2* were increased within spheroids and expressed within the T3 territory whereas, interestingly, a large number of signaling receptors were also increased.

Although Panther analysis enabled us to determine protein classes overrepresented within each territory, this approach offers no insight into the transcriptional regulation of a given territory. Understanding the regulation of a complex molecular signature provides a deeper understanding of the underlying biological process. Therefore, to identify the regulators that contribute to the activation/inactivation of our territories in the context of dermal papilla induction, we reverse-engineered a transcriptional network for whole skin using the ARACNe algorithm (39). Based on gene-expression microarrays, the network identifies all transcription factors that are expressed in whole skin and infers the direct transcriptional targets of individual transcription factors. Each transcription factor and its set of targets, known as its regulon, were subsequently interrogated to identify those transcription factors whose predicted targets are specifically enriched in the genes that demarcate each territory. Consequently, such transcription factors are candidate regulators of each territory.

Initially, we analyzed territories T1 and T3 to determine master regulators predicted to regulate genes whose expression levels are restored by spheroid culture. Using Fisher's Exact Test and Gene Set Enrichment Analysis, we interrogated the ARACNe network for regulators of three sets of genes: regulators of the T1 and T3 individually, and candidate master regulators for the combined T1 and T3 territories. Interestingly, we identified the transcription factor friend leukemia virus integration 1 (FLI1) as a unique master regulator of the combined territories T1 and T3 ($P = 2.24 \times 10^{-5}$). FLI1 was not a significant master regulator of either territory individually, but was significantly enriched in genes when these two territories were combined, and accounted for 32.5% of genes differentially regulated within these two territories (Fig. 4*F*). FLI1 is both a transcriptional activator and repressor and plays an important role in extracellular matrix production in the skin, highlighting the importance of the changing extracellular matrix profile in dermal spheroids. Despite the fact that FLI1 itself is not differentially regulated between 2D and 3D cultures, it is nevertheless predicted to be a master regulator of the T1 + T3 signature. Transcriptional expression is not the sole indicator of protein activity; moreover, one of the advantages of using the ARACNe network is that it enables detection of changes in protein activity of a transcription factor that are not detected by differential expression (40). For example, posttranslational modifications and direct regulation of the FLI1 protein may induce the differentiation program without detectable changes in FLI1 transcript expression.

Previous work had established that FLI1 negatively regulates the expression of collagens (*COL1A1* and *COL5A1*) while positively regulating the expression of genes such as *DCN* in the skin (41). Our ARACNe network of the skin enabled us to identify the regulation of the expression of these genes by FLI1, as well as the direction of regulation (up-regulated or suppressed), illustrating the power of using network-based systems analysis in understanding the regulation of large gene panels that correspond to biological processes such as hair-follicle induction. We identified a candidate regulator of a large cohort of genes that are differentially expressed upon spheroid culture, whose predicted targets and biological pathways are supported by known literature.

Although FLI1 is an interesting candidate for regulating a portion of the dermal papilla signature, it accounts only for genes already restored by 3D spheroid culture. Importantly, territories T2 and T4 contain genes that are not restored by 3D culture. To produce a fully functional dermal papilla spheroid, we postulated that it is necessary to induce the expression of the genes within these territories as well. Using our ARACNe network, we sought to identify master regulators of genes differentially expressed in territories T2, or T4, or the combined territories T2 and T4. Such regulators need not be endogenously expressed in the hair follicle. Instead, systems biology approaches are able to select molecular regulators that can be used to bypass and recapitulate a developmental process. We identified 12 predicted potential master regulators after pairing territories T2 and T4. These included ZBTB16, HCLS1, LEF1, TRIM22, and KLF11 (Fig. 4*G*). LEF1 ($P = 8.37 \times 10^{-24}$) is a predicted regulator of 24.5% of the genes in T2 and T4 (Fig. 4*G*) and is a well-known transcription factor within the Wnt signaling cascade. Additionally, HCLS1, another predicted master regulator, has been shown to be a nuclear transporter that shuttles LEF1 to the nucleus (42), underscoring the importance of Wnt signaling during hair induction (43, 44). Interestingly, ZBTB16 ($P = 3.07 \times 10^{-23}$) is required in the mouse proximal limb where it specifies mesenchymal cells required for condensation formation (45). Thus, our network analysis has identified several candidate transcription factors that together can regulate a variety of signaling pathways and developmental processes important for hair development.

Discussion

In recent years, adult human hair-follicle neogenesis has become an attractive target in regenerative medicine, in part due to the easy accessibility of follicle cells, the strong foundation of knowledge underpinning hair follicle biology, and widespread clinical interest. In this study, we first substantiated the inductive capacity of the intact human dermal papilla, by eliciting new follicle formation in recipient human skin. The inductive phenotype of dermal papilla cells is dramatically and rapidly perturbed by growth in a 2D culture microenvironment, which alone leads to a loss of inductive competence. Here, we demonstrated that this loss of inductivity is partially reversible if the cells are reassembled into 3D spheroids. We performed global profiling of cultured cells and dermal papilla spheroids compared with intact papillae, to identify the signature that underlies the inductive phenotype of the dermal papilla.

Oliver (8) first demonstrated that intact rodent papilla have inductive potential, and subsequently, the experiments demonstrating that cultured rodent papilla cells are inductive were performed by us (C.A.B.J.) in the early 1980s (9). In the late 1990s, we demonstrated that intact human dermal sheath was inductive in human skin (14) whereas, more recently, the inductive properties of intact human dermal papilla were exhibited when they were recombined with bulge-derived epithelial cells, isolated from human hair follicles (46). Nevertheless, despite intense interest, until now, the same claim could not be made for cultured human dermal papilla because they have previously been shown to induce only chimeric human/rodent hair follicles in recipient rodent tissues, and not entirely human hair follicles (19, 47). Here, we demonstrate that cultured human dermal papilla spheroids are capable of inducing de novo hair follicles in intact recipient human skin.

Growth of cells within a spheroid enabled us to facilitate cellular aggregation, which is already common in rodent cell cultures, but otherwise absent in nearly all human dermal papilla cell cultures (48). Just as dispersal of condensates during development leads to a disruption of hair-follicle morphogenesis (2), we previously postulated that loss of cell–cell cohesion in vivo in the adult can lead to papilla miniaturization and androgentic alopecia (49). Both of these scenarios have parallels with our observations here, where the condensed cells demonstrate an ability to instruct hair growth, whereas this property is absent from monolayer cultures. Although condensation of dermal papilla cells using spheroid culture is necessary, it alone is not sufficient to initiate induction because two of the seven cell lines in our study failed to promote neohairs in recipient skin. Moreover, hair follicles that did grow were small and often failed to produce hair fibers that exited the skin surface, suggesting that, after follicle initiation, the spheroid no longer elicits hair growth. The lack of sebaceous glands within spheroid-induced hair follicles also indicates that complete follicle induction has not occurred. Nevertheless, within our system, the aggregation of papilla cells in a 3D spheroid enabled partial reprogramming, which in itself was sufficient to initiate hair follicle induction in recipient human tissue. Importantly, as demonstrated when using the murine patch assay (47, 50), dermal spheroids are capable of responding to reciprocal signals from the adjacent epithelium. It is in this context that final reprogramming to a dermal papilla likely occurs. Moreover, as dermal spheroids exhibit the behavioral characteristics of intact dermal papillae, they are potentially far more useful than monolayer cultures. For example, in drug discovery (51), papilla spheroids would be effective to identify factors that alter papilla cell function, either to promote or inhibit hair growth, as studies using monolayered cultures have been hampered by their inability to consistently respond to treatments (52). Moreover, dermal spheroids may be beneficial to predict clinical response to hair-loss treatments that target the dermal papilla, providing a useful tool for precision medicine approaches. We postulate that the intrinsic variability observed in spheroids reflects the donor from which the cells were originated. We do not have additional demographic information about the donors in this study; however, we do know that they all have androgenetic alopecia. The degree of severity may be an important factor underlying inherent differences between donors. Future work will aim to determine the basis of this individual variation and whether a specific molecular signature can be identified in spheroid cultures that would be predictive of success in subsequent transplantation.

Growth of dermal papilla cells in spheroids also paves the way for rapid advances within this field, including hair-restoration applications or in cases where limited hairs are available for use as donor material, such as in scarring alopecias or burns. If we can activate spheroids to induce sebaceous glands and externalized hairs, a single follicle papilla can theoretically be used for generating a large number of spheroids, thereby allowing the regeneration of unlimited new hairs within intact recipient human tissues. Growth of hair follicles in engineered skins will also transform the skin-transplantation field, where current skin replacement models are devoid of hair follicles, and only act as a covering for a severe burn or wound. This restoration of papilla cell function invites comparison with other model systems where spheroid cultures are favored over 2D models. Particularly in the cancer research community, 3D culture models are extensively used, as they exhibit characteristics of intact tumor tissues, making them superior over 2Dly cultured cells with respect to analysis of cellular invasion and response to therapeutics (53, 54).

Why do human dermal papilla spheroids uniquely regain their inductive potential whereas dissociated cells do not? Although dermal papillae play a complex role in hair-follicle induction and cycling, they are relatively simple structures, consisting of a predominant single cell type in spherical or pear-shaped aggregates within a complex extracellular matrix. Creating papilla spheroids, therefore, very closely mimics basic dermal papilla morphology while also restoring microenvironmental cues. Furthermore, although our analysis uncovered an overrepresentation of several protein classes within spheres, the most significantly overrepresented terms related to extracellular matrix synthesis,

emphasizing that spheroids adopt the histomorphology of intact papillae. Moreover, the identification of FLI1 as a candidate master regulator of the T1 and T3 territories points to the importance of the extracellular matrix in defining a transcriptional signature within spheroids. It is noteworthy that the culture medium of our 2D and 3D cultures is the same, and we did not add any exogenous growth factors to the spheroid cultures to promote inductivity. Therefore, papilla cells are undergoing cell-intrinsic reprogramming when grown as spheroids, in part by generating their own extracellular matrix, or growth factors, and enhancing/enabling intercellular communication.

In addition to providing mechanical stability, extracellular matrix enables communication and interaction between cells. Chromatin remodeling and tissue-specific gene expression have been linked with increased extracellular matrix expression within 3D cultures (55). The dramatic difference in the collective character of papilla cells when switched from monolayer culture to aggregates also has an intriguing parallel in embryology with a phenomenon called the "community effect" (56). The community effect occurs when groups of cells use close contact interactions to establish and maintain their collective identity and has been shown experimentally to be required for specific inductive changes to occur (57).

Collective data suggest that restoring a fully functional dermal papilla spheroid to induce follicles will require more than just physical manipulation of dermal papilla cells. Of interest is a recent study where the authors demonstrated that subdermal injection of Wnts into balding scalp could reactivate hair growth, presumably by reactivating signaling networks in the latent dermal papilla (58). These latent papillae may show similar characteristics to dermal spheroids, which are devoid of any external environmental influence. Complete reactivation of dermal papilla cells likely requires cell nonautonomous communication, whether from the epidermis, surrounding adipocytes, or elsewhere in the follicle macroenvironment, not unlike the requirement for this type of communication during the hair cycle (59). Each of these environmental cues has the potential to translate to genetic changes in the hair follicle and dermal papilla. We postulate that the T2 and T4 territories correspond to molecular programs that are initiated by non-cell-autonomous environmental cues, explaining lack of a full signature restoration in 3D culture.

Using network-based methods, we aimed to artificially recapitulate the environmental requirements by identifying endogenous regulators that could mimic the environmental signals. We studied territories T2 and T4 in this context to identify regulators that may be able to bypass the environmental cues and identified 12 potential regulators that may act in this capacity. We hypothesize that a combination of these or other regulators is sufficient to confer full inductivity to dermal papilla spheroids. It is unknown how many of these regulators are expressed within dermal papilla cells; however, network analysis predicts that these transcription factors are the most parsimonious regulators of the signatures in T2 and T4. These master regulators may not have biological relevance to the hair follicle itself; nevertheless, we predict that they may be able to bypass the natural inductive program, to artificially restore the signatures of genes in T2 and T4.

In conclusion, we have demonstrated that adult human hair-follicle dermal papilla cells can be partially reprogrammed to become capable of inducing hair-follicle neogenesis simply by manipulating their cellular microenvironment. This partial reprogramming in itself is sufficient to initiate hair-follicle neogenesis in non-hair-bearing human skin; however, we have identified several additional transcriptional regulators that we predict will enable complete recapitulation of the genetic profile of a fully functioning dermal papilla. These findings represent a significant advance within the field of tissue engineering as it relates to cellular therapy of the skin and hair follicle.

Over many decades, a large body of literature has demonstrated that epithelial–mesenchymal interactions result in secondary induction and organ development. Here, we show a dramatic example of how organ neogenesis can be achieved by exploiting the inherent properties of interacting cells to create new structures. We show that it is possible to harness the inductive properties of adult cells to direct de novo organogenesis and translate this concept to demonstrate that cultured human dermal papilla cells can instruct and initiate human hair-follicle induction. Although further work will be required to increase the efficiency of this process, this crucial first step represents a milestone advance for bioengineering of human hair.

Materials and Methods

Human Dermal Papilla Isolation and 2D Cell Culture. Intact dermal papillae were isolated from occipital scalp follicles, taken from tissue obtained during hair transplantation surgery. Occipital scalp samples were obtained as discarded tissue during hair transplantation surgery, and so were designated as nonhuman subject research under 45 CFR Part 46. We therefore received an Institutional Review Board exemption at Columbia University to use these materials. Follicles were transected just above the level of the dermal papilla to isolate end bulbs, which were inverted using 27G needles to remove the matrix and expose the dermal papilla. Papilla were then separated from the follicle by cutting through their stalk. For culture, 6–8 papillae were transferred to 35-mm dishes containing 20% (vol/vol) FBS in dMEM, with 1x penicillin, streptomycin, and fungizone. Papillae were adhered to the base of the dish using a needle, and after 1 wk cells could be observed migrating out of the attached papillae. The intact papillae eventually collapsed, and, when the dish was approaching confluence, cells were passaged at a 1:2 ratio using 0.5% trypsin-edta to detach. After the initial 2 wk of culture, cells were grown in 10% (vol/vol) FBS in dMEM, with no antibiotics or antimycotics.

Establishment and Maintenance of Dermal Papilla Cells in 3D Cultures. To establish spheroids, dermal papilla cells were first split at an 80:20 ratio. It is critical that cells are grown without antibiotics at this stage. Two days post passage, cells that were seeded at 80% confluency were trypsinized for making spheroids (p3/p4/p5). Cells were centrifuged and resuspended in 5 mL of dMEM containing 10% (vol/vol) FBS for quantification. They were centrifuged a second time and resuspended at 300 cells per μL. Hanging drops were established on the lid of a Petri dish, spaced evenly apart and consisting of 3,000 cells in 10-μL volumes of dMEM/10%FBS. PBS was placed to completely cover the base of the Petri dishes, and dishes were stacked in the incubator (37 °C, 5% CO_2). After 24 h, spheroids were visible within the drops. Spheroids were then used in grafting experiments 30–48 h after hanging drops were established.

Molecular Profiling and Statistical Analysis. ***Microarray analysis.*** RNA was extracted from freshly isolated occipital scalp dermal papillae, dermal papilla cells in culture at increasing passages (p0, p1, p3, p5) 3 d post feeding, or dermal spheroids 48 h after their establishment. RNA was isolated at all experimental time points from three male donors (ages 32, 34, and 37; donors D5, D6, and D7) using a Qiagen mRNA micro kit specifically for the extraction of small amounts of RNA (required for the intact dermal papilla samples). We used the two-cycle 3′IVT amplification kit from Affymetrix for generation of biotin-labeled cRNA. Manufacturers' protocols were followed during all steps, and samples underwent two rounds of IVT amplification to establish the required 15 μg of cRNA that was used for fragmentation. Fragmented cRNA was taken to the Genomics Core facility at Columbia University, where samples were hybridized onto Affymetrix U133 plus 2.0 genechips and analyzed using an Affymetrix GeneChip system. Data output from the microarray analysis was in the form of CEL files.

GeneSpring. We used the commercially available software GeneSpring to analyze our datasets. The array data were preprocessed using Robust Multiarray analysis (RMA) to perform background correction, normalization, and summarization followed by a baseline transformation (baseline to median of all samples) to generate "normalized" values. Expression levels that are output have been log2 transformed. We filtered normalized values based on their expression, using a lower 20% cutoff. We used a one way ANOVA to identify differentially expressed genes, and, coupled with a Benjamini–Hochberg multiple testing correction, performed paired comparisons between cells at different stages in culture respective to intact papilla. We also compared individual data points, such as freshly isolated papilla versus p0

cells, or p3 cells versus spheroids. Here, we used an unpaired two-sample *t* test, coupled with a Benjamini–Hochberg multiple testing correction to establish significant entities ($P < 0.05$). We then filtered lists based on a differential cutoff above or below 2 to obtain gene lists of interest.

The gene list comparing intact papillae with cells at p3 was used for correlation analysis. RMA normalized and log2-transformed values were obtained for every transcript (6,259). The similarity between intact papillae and p3 cells, or intact papilla and spheroids, was expressed as Pearson's correlation coefficient using the R package. Correlation was calculated for individual datasets, obtained from three separate donors. Error bars were based on ninety-five percent confidence intervals on r, which were calculated by transformation of r to a normal sampling distribution (*z*), and back-transforming the SE of *z*.

GeneCluster. Unsupervised hierarchical clustering was performed on all array samples to see how samples align by donor and stage in culture. Median normalized data (before filtering) were input into GeneCluster 3.0, filtered so at least one observation contained an absolute value >0.5, resulting in a list of 47,367 transcripts for clustering. Data were log2 transformed and hierarchically clustered using Pearson's uncentered correlation coefficient with average linkage.

iPAGE. We used RMA preprocessed (but not baseline-transformed) data values for every entity represented on the U133 plus 2.0 genechip for three replicates of intact dermal papilla, and three replicates at p0. Data were median-normalized, against the median of each array replicate, and values were averaged across all three replicates for an experimental condition. We calculated the log2 value of the ratio of expression values between cultured cells at p0, and intact papillae. The log2 values were input into the iGET algorithm, and iPAGE was specifically selected for continuous analysis. Default parameters were used for analysis whereas the expression bin count was set at 20. iPAGE uses an information theoretic algorithm to identify pathways and cellular processes that are deregulated between intact papillae and cultured cells.

GEDI. Dynamic data analysis was performed using GEDI. Normalized expression values, for every probeset and each sample, were generated in GeneSpring and input into GEDI for analysis. GEDI uses a Self Organizing Map (SOM) algorithm to cluster transcripts into metagenes, based on their similar expression pattern across donors and cell-culture conditions. Six hundred fifty metagene tiles are established during the analysis on a 25 × 26 grid. The changing dynamics of each metagene can then be assessed as they change during culture and subsequent sphere formation. Metagenes can be clustered into territories for further analysis.

Panther. We established that 22% of genes differentially regulated from intact papillae, by growth in culture, were restored by growth as spheroids. This 22% equates to 1,351 transcripts that either increase (UP) or decrease (DOWN) contributing to restoration of an intact signature. We used Panther gene-expression tools for analysis of the UP and DOWN categories for both the 22% of genes and those identified in T1 or T3 territories during the GEDI analysis. Panther categorizes genes into either pathways, gene ontology classes, or protein classes and calculates representation of a particular term, such as protein class (within a given gene list), and compares it to representation of that term within the homo sapiens genome to look for overrepresentation.

ARACNe. The ARACNe algorithm is an information theoretic method of inferring transcriptional interactions using gene-expression array data (39). It attempts to identify transcription factor–transcription target interactions using mutual information, a nonparametric measure of statistical dependence that is not tied to correlation. This approach has been previously applied to study master regulators in the context of glioblastoma and B-cell lymphoma (60–62) and has proven more sensitive than traditional statistical metrics of correlation. To use the ARACNe algorithm, we first assembled a skin database, consisting of a cohort of 128 Affymetrix U133 Plus 2.0 gene-expression microarrays that were GCRMA normalized together. Arrays were compiled from other projects ongoing within our laboratory and consisted of both whole-skin biopsies of normal or diseased tissue and skin (dermal and epidermal) primary cell cultures. We then implemented ARACNe to reconstruct transcriptional networks within the skin database, establishing a skin-specific transcriptome. Direct transcriptional targets for each transcription factor in the skin transcriptome are identified by the algorithm via the application of the Data Processing Inequality (DPI). The transcriptional network produced consists of transcription factors and their direct predicted transcriptional targets. We sought to identify master regulators of gene territories previously established during the GEDI analysis. We therefore interrogated the skin transcriptome for panel enrichment and associations of differential expression using both Fisher's Exact Test and Gene Set Enrichment Analysis (58), to identify transcription factors with an enriched set of targets within a particular territory. We assessed six combinations of territories: T1–T4 by themselves, and also T1 + T3 or T2 + T4 combined, to identify candidate master regulators.

Real-Time PCR and Statistical Analysis. cDNA was generated from RNA samples (F, p0, p1, p3, p5, S from three male donors D5, D6, and D7) following Invitrogen protocols and using SuperScript III with a mixture of random hexamers and oligo dT primers. Semiquantitative PCR was performed using Sybr Green PCR mix on an Applied Biosystems 7300 Real-Time PCR System. Primers for beta 2 microglobulin were used in each reaction as a baseline control. Fold changes were calculated using the delta-delta CT algorithm, relative to beta 2 microglobulin. Samples to which comparisons were made were set as a baseline value of 1. Error bars were calculated based on SD across three technical replicates within one biological replicate. An unpaired two-tailed *t* test was used to calculate whether differences between samples, across three technical replicates, were significant, or $P < 0.05$. Biological replicates were performed for each gene of interest and always showed similar trends whereas exact fold changes were variable.

Immunofluorescence Analysis. Cultured dermal papilla cells or spheroids sectioned on a cryostat were fixed using either 4% (wt/vol) paraformaldehyde fixation for 10 min, or methonal-acetone (1:1) fixation at −20 °C for 7 min. Cells were permeabilized for 10 min using PBS with 0.5% Triton X-100. Blocking was performed for 1 h using 2% (wt/vol) Fish Skin Gelatin in PBS. The following primary antibodies were used; rabbit anti-Periostin (1:50; Abcam), rabbit anti-HAS2 (1:50; Biorbyt), rabbit anti-BMP2 (1:50; Abcam), rabbit anti-SFRP2 (1:100; Abgent), rabbit anti-MGP (1:50; Abgent), and rabbit anti-A2M (1:200; Neobiolab). Antibodies were left overnight at 4 °C. The next day, primary antibodies were washed off using three consecutive PBS washes. A secondary antibody, Alexafluor 488 donkey anti-rabbit (1:800; Molecular Probes) was applied for 1 h at room temperature. Coverslips were mounted using Vectasheild containing DAPI (Vector Labs), and slides were visualized on a Zeiss Exciter confocal microscope.

Human-to-Human Inductive Assay. We obtained foreskins as discarded tissue after circumcision from the Children's Hospital at Columbia University Medical Center. Samples were designated as nonhuman subject research under 45 CFR Part 46, and we therefore received an Institutional Review Board exemption at Columbia University to use these materials. Foreskins were trimmed to remove excess dermal tissue and cut into 7mm × 7mm squares. They were laid on a drop of 5mg/mL dispase in HBSS for 35 min at room temperature and then moved to a Petri dish containing dMEM with 1× penicillin, streptomycin, and fungizone to wash for 2 h. Skins were partially split at the basement membrane zone, by peeling the epidermis back over the dermis. Separated skins were transferred onto a 35-mm dish containing a gel of 1% Geys Agar, 5% (vol/vol) FBS in dMEM with 1× penicillin, streptomycin, and fungizone. Intact papillae (two donors), a papilla cell slurry (two donors), or papilla spheroids (seven donors) were placed onto the exposed dermis, and the epidermis was peeled back over to cover them. Skins were left to recombine overnight at 37 °C before grafting.

Recombined skins were grafted onto the back of 8- to 10-wk-old SCID mice, obtained from Taconic. All work was approved by the Institutional Animal Care and Use Committee at Columbia University. Eight-millimeter-diameter pieces of skin were removed from the dorsal side of mice by using the pinch-tent technique for cutting. Foreskin was laid epidermal side up onto the exposed fascia and kept in place using interrupted 7–0 nylon sutures. Mouse skin that was removed was decellularized by freeze thawing three times and then sutured back into place over the top of the foreskin graft. Grafts were bandaged using Opsite Flexfix for 3 wk, after which time bandages and sutures were removed and mice were kept under normal husbandry conditions for a further 3 wk.

Hair Induction Analysis. After 6 wk, mice were sacrificed and grafts were removed. Grafts were subsequently frozen in OCT compound for analysis. Serial 7-μM sections were cut on a cryostat, and half of all sections were analyzed by hematoxylin/eosin staining. Remaining sections were used for subsequent analysis. For immunofluorescence, the following primary antibodies were used: mouse anti-human nuclei (1:100), rabbit anti-K14 (1:2,000), and chicken anti-K15 (1:1,000) (all from Chemicon); rabbit anti-laminin 5 (1:1,000; Abcam); guinea pig anti-K75 (1:2,000) and guinea pig anti-K31 (1:2,000) (both gifts from Lutz Langbein, University of Heidelberg, Heidelberg); rabbit anti-K71 (1:1,000, gift from Yutaka Shimomura, Niigata University, Niigata, Japan); and rat anti-mouse CD31 (clone 390, 1:100; ebiosciences). For alkaline phosphatase staining, slides were incubated in TN buffer before 20 min incubation with NBT:BCIP in TN buffer. Slides were washed and counterstained with eosin for improved visualization.

Hematoxylin/eosin-stained sections were laser capture microdissected into a microfuge tube with adhesive caps (Zeiss). End bulbs of induced hairs were microdissected using the auto LPC function of Palm Robot V2.2 software on a Palm MicroBeam LCM system (Zeiss). The WGA4 GenomePlex Single Cell Whole Genome Amplification Kit (Sigma) was used to isolate and amplify genomic DNA. Microsatellite markers were selected for comparative genomic analysis. PCR was performed on donor spheroid cell DNA, foreskin recipient tissue DNA, and endbulb tissue DNA to determine the contribution of donor cells in hair follicles. PCR products were separated on a 12% acrylamide gel and visualized on the Gel Logic 100 imaging system.

ACKNOWLEDGMENTS. We thank Emily Chang and Ming Zhang for excellent technical support. We are indebted to Dr. Robert Bernstein for generously providing us with tissue for this study, to Drs. Andrea Califano and Saeed Tavazoie for their expertise and helpful discussions in computational and systems biology, and to Dr. Lynn Petukhova for expert statistical advice. This study was supported by a Science of Human Appearance Career Development Award from the Dermatology Foundation (to C.A.H.), the Biotechnology and Biological Sciences Research Council (BBSRC) follow on fund, and a Medical Research Council (MRC) Grant G1000846 (to C.A. B.J.), and New York State Foundation for Science Technology and Innovation (NYSTAR) and New York State Stem Cell Science (NYSTEM) grants (to A.M.C.).

1. Pinkus H (1958) *The Biology of Hair Growth*, eds Montagna W, Ellis RA (Academic, New York), pp 1–32.
2. Jacobson CM (1966) A comparative study of the mechanisms by which X-irradiation and genetic mutation cause loss of vibrissae in embryo mice. *J Embryol Exp Morphol* 16(2):369–379.
3. Kollar EJ (1970) The induction of hair follicles by embryonic dermal papillae. *J Invest Dermatol* 55(6):374–378.
4. Dhouailly D (1973) Dermo-epidermal interactions between birds and mammals: Differentiation of cutaneous appendages. *J Embryol Exp Morphol* 30(3):587–603.
5. Millar SE (2002) Molecular mechanisms regulating hair follicle development. *J Invest Dermatol* 118(2):216–225.
6. Ito M, et al. (2007) Wnt-dependent de novo hair follicle regeneration in adult mouse skin after wounding. *Nature* 447(7142):316–320.
7. Cohen J (1961) The transplantation of individual rat and guineapig whisker papillae. *J Embryol Exp Morphol* 9:117–127.
8. Oliver RF (1970) The induction of hair follicle formation in the adult hooded rat by vibrissa dermal papillae. *J Embryol Exp Morphol* 23(1):219–236.
9. Jahoda CA, Horne KA, Oliver RF (1984) Induction of hair growth by implantation of cultured dermal papilla cells. *Nature* 311(5986):560–562.
10. Kishimoto J, Burgeson RE, Morgan BA (2000) Wnt signaling maintains the hair-inducing activity of the dermal papilla. *Genes Dev* 14(10):1181–1185.
11. Rendl M, Polak L, Fuchs E (2008) BMP signaling in dermal papilla cells is required for their hair follicle-inductive properties. *Genes Dev* 22(4):543–557.
12. Cooley J (2004) Follicular cell implantation: An update on "hair follicle cloning" *Facial Plast Surg Clin North Am* 12(2):219–224.
13. Teumer J, Cooley J (2005) Follicular cell implantation: An emerging cell therapy for hair loss. *Semin Plast Surg* 19(2):194–200.
14. Reynolds AJ, Lawrence C, Cserhalmi-Friedman PB, Christiano AM, Jahoda CA (1999) Trans-gender induction of hair follicles. *Nature* 402(6757):33–34.
15. Jahoda CA, et al. (2001) Trans-species hair growth induction by human hair follicle dermal papillae. *Exp Dermatol* 10(4):229–237.
16. Reynolds AJ, Jahoda CA (1996) Hair matrix germinative epidermal cells confer follicle-inducing capabilities on dermal sheath and high passage papilla cells. *Development* 122(10):3085–3094.
17. Ouji Y, Nakamura-Uchiyama F, Yoshikawa M (2013) Canonical Wnts, specifically Wnt-10b, show ability to maintain dermal papilla cells. *Biochem Biophys Res Commun* 438(3):493–499.
18. Ohyama M, Kobayashi T, Sasaki T, Shimizu A, Amagai M (2012) Restoration of the intrinsic properties of human dermal papilla in vitro. *J Cell Sci* 125(Pt 17):4114–4125.
19. Qiao J, et al. (2009) Hair follicle neogenesis induced by cultured human scalp dermal papilla cells. *Regen Med* 4(5):667–676.
20. Jahoda CA, Oliver RF (1984) Vibrissa dermal papilla cell aggregative behaviour in vivo and in vitro. *J Embryol Exp Morphol* 79:211–224.
21. Birgersdotter A, Sandberg R, Ernberg I (2005) Gene expression perturbation in vitro—a growing case for three-dimensional (3D) culture systems. *Semin Cancer Biol* 15(5): 405–412.
22. Higgins CA, Richardson GD, Ferdinando D, Westgate GE, Jahoda CA (2010) Modelling the hair follicle dermal papilla using spheroid cell cultures. *Exp Dermatol* 19(6): 546–548.
23. Trapp BD, Honegger P, Richelson E, Webster HD (1979) Morphological differentiation of mechanically dissociated fetal rat brain in aggregating cell cultures. *Brain Res* 160(1):117–130.
24. Shimomura Y, et al. (2010) APCDD1 is a novel Wnt inhibitor mutated in hereditary hypotrichosis simplex. *Nature* 464(7291):1043–1047.
25. Kratochwil K, Dull M, Farinas I, Galceran J, Grosschedl R (1996) Lef1 expression is activated by BMP-4 and regulates inductive tissue interactions in tooth and hair development. *Genes Dev* 10(11):1382–1394.
26. Goodarzi H, Elemento O, Tavazoie S (2009) Revealing global regulatory perturbations across human cancers. *Mol Cell* 36(5):900–911.
27. Andl T, Reddy ST, Gaddapara T, Millar SE (2002) WNT signals are required for the initiation of hair follicle development. *Dev Cell* 2(5):643–653.
28. Schmeichel KL, Bissell MJ (2003) Modeling tissue-specific signaling and organ function in three dimensions. *J Cell Sci* 116(Pt 12):2377–2388.
29. Eichler GS, Huang S, Ingber DE (2003) Gene Expression Dynamics Inspector (GEDI): For integrative analysis of expression profiles. *Bioinformatics* 19(17):2321–2322.
30. Greco V, et al. (2009) A two-step mechanism for stem cell activation during hair regeneration. *Cell Stem Cell* 4(2):155–169.
31. Rendl M, Lewis L, Fuchs E (2005) Molecular dissection of mesenchymal-epithelial interactions in the hair follicle. *PLoS Biol* 3(11):e331.
32. Ito Y, et al. (2007) Isolation of murine hair-inducing cells using the cell surface marker prominin-1/CD133. *J Invest Dermatol* 127(5):1052–1060.
33. Närhi K, et al. (2012) Sostdc1 defines the size and number of skin appendage placodes. *Dev Biol* 364(2):149–161.
34. van Genderen C, et al. (1994) Development of several organs that require inductive epithelial-mesenchymal interactions is impaired in LEF-1-deficient mice. *Genes Dev* 8(22):2691–2703.
35. Clavel C, et al. (2012) Sox2 in the dermal papilla niche controls hair growth by fine-tuning BMP signaling in differentiating hair shaft progenitors. *Dev Cell* 23(5): 981–994.
36. Kulessa H, Turk G, Hogan BL (2000) Inhibition of Bmp signaling affects growth and differentiation in the anagen hair follicle. *EMBO J* 19(24):6664–6674.
37. Plikus MV, et al. (2008) Cyclic dermal BMP signalling regulates stem cell activation during hair regeneration. *Nature* 451(7176):340–344.
38. Thomas PD, et al. (2003) PANTHER: A browsable database of gene products organized by biological function, using curated protein family and subfamily classification. *Nucleic Acids Res* 31(1):334–341.
39. Margolin AA, et al. (2006) ARACNE: An algorithm for the reconstruction of gene regulatory networks in a mammalian cellular context. *BMC Bioinformatics* 7(Suppl 1):S7.
40. Lefebvre C, et al. (2010) A human B-cell interactome identifies MYB and FOXM1 as master regulators of proliferation in germinal centers. *Mol Syst Biol* 6:377.
41. Asano Y, et al. (2009) Transcription factor Fli1 regulates collagen fibrillogenesis in mouse skin. *Mol Cell Biol* 29(2):425–434.
42. Skokowa J, et al. (2012) Interactions among HCLS1, HAX1 and LEF-1 proteins are essential for G-CSF-triggered granulopoiesis. *Nat Med* 18(10):1550–1559.
43. Chen D, Jarrell A, Guo C, Lang R, Atit R (2012) Dermal β-catenin activity in response to epidermal Wnt ligands is required for fibroblast proliferation and hair follicle initiation. *Development* 139(8):1522–1533.
44. Myung PS, Takeo M, Ito M, Atit RP (2013) Epithelial Wnt ligand secretion is required for adult hair follicle growth and regeneration. *J Invest Dermatol* 133(1):31–41.
45. Barna M, Pandolfi PP, Niswander L (2005) Gli3 and Plzf cooperate in proximal limb patterning at early stages of limb development. *Nature* 436(7048):277–281.
46. Toyoshima KE, et al. (2012) Fully functional hair follicle regeneration through the rearrangement of stem cells and their niches. *Nat Commun* 3:784.
47. Kang BM, Kwack MH, Kim MK, Kim JC, Sung YK (2012) Sphere formation increases the ability of cultured human dermal papilla cells to induce hair follicles from mouse epidermal cells in a reconstitution assay. *J Invest Dermatol* 132(1):237–239.
48. Messenger AG, Senior HJ, Bleehen SS (1986) The in vitro properties of dermal papilla cell lines established from human hair follicles. *Br J Dermatol* 114(4):425–430.
49. Jahoda CA (1998) Cellular and developmental aspects of androgenetic alopecia. *Exp Dermatol* 7(5):235–248.
50. Huang YC, et al. (2013) Scalable production of controllable dermal papilla spheroids on PVA surfaces and the effects of spheroid size on hair follicle regeneration. *Biomaterials* 34(2):442–451.
51. Tung YC, et al. (2011) High-throughput 3D spheroid culture and drug testing using a 384 hanging drop array. *Analyst (Lond)* 136(3):473–478.
52. Messenger AG, Rundegren J (2004) Minoxidil: Mechanisms of action on hair growth. *Br J Dermatol* 150(2):186–194.
53. Nelson CM, Bissell MJ (2005) Modeling dynamic reciprocity: Engineering three-dimensional culture models of breast architecture, function, and neoplastic transformation. *Semin Cancer Biol* 15(5):342–352.
54. Lee GY, Kenny PA, Lee EH, Bissell MJ (2007) Three-dimensional culture models of normal and malignant breast epithelial cells. *Nat Methods* 4(4):359–365.
55. Spencer VA, Xu R, Bissell MJ (2010) Gene expression in the third dimension: The ECM-nucleus connection. *J Mammary Gland Biol Neoplasia* 15(1):65–71.
56. Gurdon JB (1988) A community effect in animal development. *Nature* 336(6201): 772–774.
57. Saka Y, Lhoussaine C, Kuttler C, Ullner E, Thiel M (2011) Theoretical basis of the community effect in development. *BMC Syst Biol* 5:54.
58. Zimber MP, et al. (2011) Hair regrowth following a Wnt- and follistatin containing treatment: safety and efficacy in a first-in-man phase 1 clinical trial. *J Drugs Dermatol* 10(11):1308–1312.
59. Jahoda CA, Christiano AM (2011) Niche crosstalk: Intercellular signals at the hair follicle. *Cell* 146(5):678–681.
60. Carro MS, et al. (2010) The transcriptional network for mesenchymal transformation of brain tumours. *Nature* 463(7279):318–325.
61. Basso K, et al. (2005) Reverse engineering of regulatory networks in human B cells. *Nat Genet* 37(4):382–390.
62. Mani KM, et al. (2008) A systems biology approach to prediction of oncogenes and molecular perturbation targets in B-cell lymphomas. *Mol Syst Biol* 4:169.